J Therm Anal Calorim (2012) 109:1229–1235
DOI 10.1007/s10973-012-2311-9

Novel carbon materials for thermal energy harvesting

Mark S. Romano · Sanjeev Gambhir · Joselito M. Razal · Adrian Gestos · Gordon G. Wallace · Jun Chen

NATAS2011 Conference Special Chapter

Abstract To decrease the consumption of fossil fuels, research has been done on utilizing low grade heat, sourced from industrial waste streams. One promising thermoenergy conversion system is a thermogalvanic cell; it consists of two identical electrodes held at different temperatures that are placed in contact with a redox-based electrolyte [1, 2]. The temperature dependence of the direction of redox reactions allows power to be extracted from the cell [3, 4]. This study aims to increase the power conversion efficiency and reduce the cost of thermogalvanic cells by optimizing the electrolyte and utilizing a carbon based electromaterial, reduced graphene oxide, as electrodes. Thermal conductivity measurements of the $K_3Fe(CN)_6$/$K_4Fe(CN)_6$ solutions used, indicate that the thermal conductivity decreases from 0.591 to 0.547 W/m K as the concentration is increased from 0.1 to 0.4 M. The lower thermal conductivity allowed a larger temperature gradient to be maintained in the cell. Increasing the electrolyte concentration also resulted in higher power densities, brought about by a decrease in the ohmic overpotential of the cell, which allowed higher values of short circuit current to be generated. The concentration of 0.4 M $K_3Fe(CN)_6$/$K_4Fe(CN)_6$ is optimal for thermal harvesting applications using R-GO electrodes due to the synergistic effect of the reduction in thermal flux across the cell and the enhancement of power output, on the overall power conversion efficiency. The maximum mass power density obtained using R-GO electrodes was 25.51 W/kg (three orders of magnitude higher than platinum) at a temperature difference of 60 °C and a $K_3Fe(CN)_6$/$K_4Fe(CN)_6$ concentration of 0.4 M.

Keywords Graphene · Reduced graphene oxide · Thermal conductivity · Thermal enery harvesting · Thermogalvanic Cell

Introduction

Energy, whether in the form of oil, gasoline or electricity is an essential constituent of all economic activity. An increase in population growth and demand for a more energy intensive standard of living (in 2007 the world primary energy use increased by 2.4%) has resulted in enormous strain on the global energy supply. This is made apparent by the skyrocketing of oil prices (cost per barrel: $28 in 2003, $38 in 2005 and above $80 in 2006) and the increased cost of commodities that utilize petroleum for manufacture and transport [5, 6].

Extensive research has been carried out into developing alternative energy sources. One such alternative is the harnessing of low grade heat, (temperature below 130 °C) which is usually the final product of energy conversion and in most cases, is not utilized. Examples of thermal energy sources are geothermal activity and industrial waste streams. Several thermal converters have been developed including, thermally recharged cells, thermocouples and thermionic converters [3]. However, despite the advances made for these systems, current thermoelectric conversion is hampered by high initial cost, low efficiency and material limitations [7].

One device that shows promise as a thermoenergy conversion system is a thermogalvanic cell, also known as

M. S. Romano · S. Gambhir · J. M. Razal · A. Gestos · G. G. Wallace · J. Chen (✉)
Intelligent Polymer Research Institute, ARC Centre of Excellence for Electromaterials Science, Australian Institute of Innovative Materials, University of Wollongong, Fairy Meadow, NSW 2519, Australia
e-mail: junc@uow.edu.au
URL: http://ipri.uow.edu.au/people/UOW040220.html

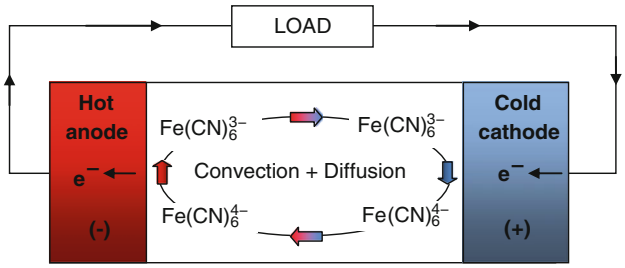

Fig. 1 Ferri/ferro cyanide redox thermogalvanic cell

a galvanic thermopile. It is an electrochemical system that consists of two electrodes (usually identical) that are held at different temperatures and placed in contact with a redox-based electrolyte [1, 8]. It utilizes the temperature dependence of the direction of redox reactions to generate a potential difference, such that when the cell is connected to an external circuit, current and power can be extracted [3]. Various electrolytes have been used for galvanic thermopiles: molten salt electrolytes, solid electrolytes and aqueous electrolytes [9]. A schematic of a thermogalvanic cell using a ferri/ferro cyanide redox couple is shown in Fig. 1 below.

For the cell shown, electrons are donated at the anode during oxidation of ferrocyanide which then travels through an external circuit. These move back to the cell via the cathode where they are consumed during the reduction of ferricyanide [4]. The electrolyte composition is maintained by the balance of oxidized and reduced species; i.e. for each mole of ferrocyanide being oxidized an equivalent number of moles of ferricyanide are being reduced. Diffusion and convection will prevent the accumulation of reaction products at each electrode and allow the cell to operate in a self-regenerative way.

The merits of this cell are its maintenance free operation, lack of moving mechanical components, direct conversion of thermal to electric energy, zero carbon emission and stability over extended periods. However, thermogalvanic devices are not without their limitations. Past studies revealed power conversion efficiencies within the range of 0.08–0.6% relative to that of a Carnot engine. These values are unacceptable for commercialization. Platinum electrodes can be utilized to achieve appreciable efficiencies; however, the high cost renders it unsuitable for practical applications [10].

A two dimensional material that has been attracting interest in the scientific community is graphene. It consists of a single layer of carbon atoms bonded in a hexagonal lattice. Research on this promising nanomaterial reveals that it has superb thermal, mechanical and electrical properties [11–14]. The attractive characteristics of graphene for electrochemical applications are its charge carrier mobility of 200,000 cm^2/V s and specific surface area of 2,630 m^2/g [15, 16]. Graphene was first fabricated by chemical vapour deposition in the 1970s [17] but it was not until recently that real progress was made in this area. Novoselov et al. [18] discovered that micromechanical exfoliation, also known as the 'scotch tape' method allowed monolayers to be peeled from graphite crystals resulting in pristine graphene. Although the graphene obtained was defect free this method had one disadvantage which is very low yield and throughput. In order to facilitate large scale production of graphene, methods for the exfoliation of graphite in the liquid phase (via chemical conversion or surfactant/solvent stabilization) have been developed [19, 20], resulting in graphene-like materials, such as reduced graphene oxide (R-GO).

This study aims to increase the power conversion efficiency and reduce the cost of thermogalvanic cells by optimizing the electrolyte ($K_3Fe(CN)_6/K_4Fe(CN)_6$) and utilizing a carbon based electromaterial, in-house synthesized reduced R-GO.

Experimental

R-GO synthesis

Graphene oxide (GO) was synthesized using a modified Hummers method, wherein natural graphite was subjected to a preoxidation step to avoid particles that had a graphite oxide shell and graphite core. 15 ml concentrated H_2SO_4, 5 g $K_2S_2O_8$ and 5 g P_2O_5 were mixed in a three neck round bottom flask that was immersed in an oil bath. The temperature was then raised to 80 °C after which 10 g of Bay Carbon natural graphite powder was added. The reaction was kept at 80 °C for 20 min then allowed to cool to room temperature. The mixture was then washed with de-ionized water and filtered until the filtrate was pH neutral; the resulting filtrand being preoxidized graphite.

230 ml of H_2SO_4 was placed in a round bottomed flask and cooled, using an ice and water bath, to 0°C. The preoxidized graphite was then added followed by 30 g $KMnO_4$ (these were added slowly so as not to raise the temperature above 20 °C). The temperature was then raised to 35 °C and maintained for 2 h. 460 ml of de-ionized water was then added very slowly to prevent an excessive rise in temperature after which it was allowed to cool to room temperature. 1,400 ml of de-ionized water was added followed by 25 ml of 30% H_2O_2, changing the colour of the mix to a bright yellow. The mix was left for 15 min after which it was centrifuged at 3,500 rpm for 30 min (Sigma 4-15). The sediments were collected and mixed with 3,650 ml of 1:10 diluted conc. HCl solution for 15 min then centrifuged at 3,500 rpm for 30 min. The sediments were collected and mixed with water followed

by centrifuge at the same speed. This step was repeated until the pH of the supernatant reached a value of 4; wherein the resulting sediment is graphite oxide.

A 200 ml suspension of graphite oxide having a concentration of 0.5 wt% was prepared and subjected to exfoliation for 2 h using 8 s on/off pulses with a probe sonicator (Branson Probe Sonifier) resulting in GO. The volume was then diluted to 2 l to make a 0.05 wt% GO dispersion and subjected to exfoliation for 2 h using the same pulse settings. 400 µl of hydrazine, 6 ml of ammonia and 50 ml of H_2O were mixed then added to the GO dispersion after which the temperature was raised to 90 °C and left for 40 min with constant stirring. The resulting R-GO dispersion was then allowed to cool to room temperature.

Thermal harvesting

Thermal harvesting experiments were carried out using a in-house designed U-shaped cell with a separation distance of 10 cm, wherein one half-cell was cooled using circulating liquid and the other was heated using an Omegalux Rope Heater (accuracy ± 1 °C) hooked up to a TCA control box that has 48 × 48 controller with PID control action and 25 A solid state relay. A schematic of the cell is shown in Fig. 2.

The temperature difference between the two sides was varied from 10 to 60 °C at 10 °C intervals. Teflon PFA coated thermocouple probes were positioned beside the electrodes to monitor the temperature in both sides of the cell. The R-GO dispersion was subjected to vacuum filtration and the resulting film was sampled to give electrodes that were 1.5 × 0.5 cm^2 and approximately 1.8 µm thick.

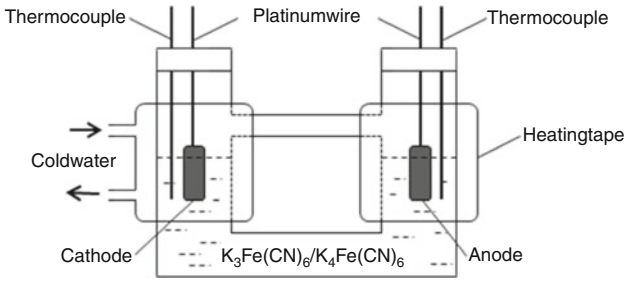

Fig. 2 Schematic of the U-shaped cell used

The electrolyte used was $K_3Fe(CN)_6/K_4Fe(CN)_6$ in aqueous media with concentrations of 0.1, 0.2, 0.3 and 0.4 mol/l. Short circuit current density and open circuit voltage were measured using an Agilent 34410A Multimeter.

Characterization

The thermal conductivity of the $K_3Fe(CN)_6/K_4Fe(CN)_6$ solutions was measured in air using a C-Therm TCi Thermal Conductivity Analyzer (C-Therm Technologies Ltd., Canada) [21]. The viscosity and electrical conductivity of the electrolyte was measured using an AR-G2 Rheometer and a TPS smartCHEM-Lab, respectively. Ultra violet–Visible spectroscopy (UV–Vis) was carried out on the GO and R-GO dispersions using a Shimadzu UV-3600. Sheet resistance measurements were taken using a JANDEL RM3 four point probe. Thermogravimetric analysis (TGA) was done on the GO and R-GO samples in air with a heating rate of 2 °C/min from room temperature to 900 °C using a TA Instruments Q500 TGA. The morphology of the films was investigated using a JEOL JSM-7500FA field emission scanning electron microscope.

Results and discussion

The produced R-GO films had a thickness of 1.8 µm and a sheet resistance of 219.11 Ω/Square. Reduction of GO using hydrazine restored the electronic conjugation within the R-GO sheets as indicated by the redshift of the absorption peak in the UV–Vis (Fig. 3a) of R-GO (267 nm) compared to GO (232 nm). TGA curves (Fig. 3b) of GO (sample mass: 0.395 mg) indicate a weight loss of 30.11% around 200 °C which is caused by the pyrolysis of the oxygen containing functional groups forming CO, CO_2 and steam. Reduction of GO with hydrazine removed the oxygen containing functional groups which is evident in the lack of weight loss at 200 °C for the TGA curves of R-GO (sample mass: 0.465 mg) [22, 23]. R-GO also displays an abrupt mass loss at 548.8 °C, wherein 83.83% of the sample decomposes. GO, on the other hand starts decomposing at 410.8 °C, almost 40 °C earlier than R-GO. This disparity can be attributed to the difference in structure for these two carbon

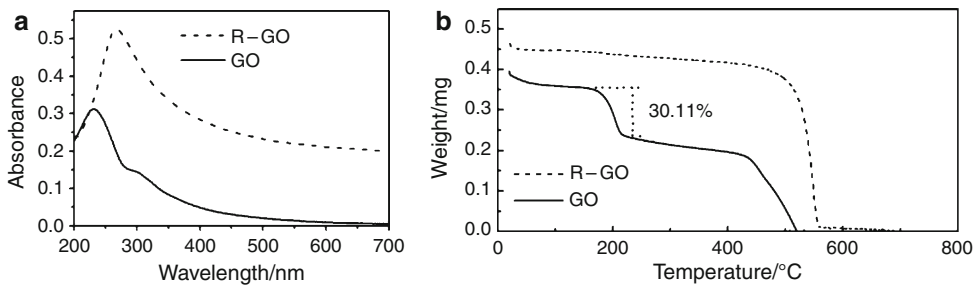

Fig. 3 **a** UV–Vis spectra. **b** TGA curves of the GO and R-GO samples

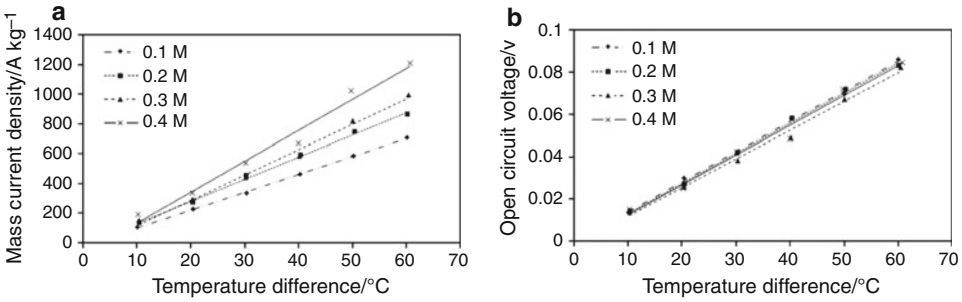

Fig. 4 **a** Mass current density. **b** Open circuit voltage at different concentrations of $K_3Fe(CN)_6/K_4Fe(CN)_6$

materials. The oxygen containing functional groups in GO diminish the integrity of the sp^2 system which lowers its thermal stability and also leads to total decomposition. Hydrazine reduction in R-GO restores the sp^2 system which leads to its higher thermal stability [24].

Thermal harvesting experiments reveal that the mass current density (I_d) scales with the concentration of $K_3Fe(CN)_6/K_4Fe(CN)_6$, wherein a maximum value of 0.195 mA was obtained at 0.4 M (the saturation point) as shown in Fig. 4a. This rise in I_d is brought about by a decrease in the ohmic overpotential of the cell, the dominant contributor to the cell resistance [10] and an increase in the species available to carry out the redox reactions required to generate the short circuit current.

The open circuit voltage (V_{oc}) does not vary much with electrolyte concentration as shown in Fig. 4b and has an average value of 83.88 mV giving a Seebeck coefficient of 1.39 mV/K, which is in good agreement with literature [25]. This relationship between the Seebeck coefficient and electrolyte concentration is expected since the amounts of redox mediator used was equimolar and the Seebeck coefficient is dictated by the thermodynamics of the redox couple as given by:

$$S = \frac{\Delta V}{\Delta T} = \frac{S_B - S_A}{n\mathrm{F}} \tag{1}$$

where S is the Seebeck coefficient of a hypothetical redox couple $A \leftrightarrow ne^- + B$, ΔV represents the electrode potential, ΔT is temperature difference between electrodes, S_A and S_B are the partial molar entropies of species A and B, respectively, n is the number of electrons involved in the redox reaction and F is Faraday's constant [3].

The power conversion efficiency (Φ) of a thermogalvanic cell is given by

$$\Phi = \frac{\text{Electrical power output}}{\text{Thermal power flowing through the cell}} \tag{2}$$

The electrical power output is maximal under conditions of equality of external load resistance and internal resistance of the cell [26]. This may be obtained from plots of the open circuit potential (V_{oc}) versus short circuit current (I_{sc}) that is delivered by the cell and is given by $0.25V_{oc}I_{sc}$. The thermal power flowing through a cell, wherein there is no net consumption of electrolyte, i.e. for systems using reversible redox couples, is given by $KA(\Delta T/d)$, where K is the thermal conductivity of the electrolyte, A is the cross sectional area of each electrode and $\Delta T/d$ is the temperature gradient across the distance between the two electrodes [27]. This allows Eq. 2 to be expressed as:

$$\Phi = \frac{0.25V_{oc}I_{sc}}{KA(\Delta T/d)} \tag{3}$$

Using Eq. 3, power conversion efficiency at the various electrolyte concentrations were calculated and are presented in Fig. 5, which indicates that higher power conversion efficiency values are obtained at higher concentration of the redox mediator. The highest value obtained for the thermal cell was 0.00825% at an electrolyte concentration of 0.4 M.

One reason for the improved efficiency is that an increase in concentration of the redox mediator results in lower thermal conductivity as shown in Fig. 5. Despite the fact that an increase in temperature causes the thermal conductivity of the $K_3Fe(CN)_6/K_4Fe(CN)_6$ solutions to rise at roughly the same rate, as depicted in Fig. 6a, a concentration of 0.4 M still has the most desirable thermal conductivity for applications as the electrolyte in thermal

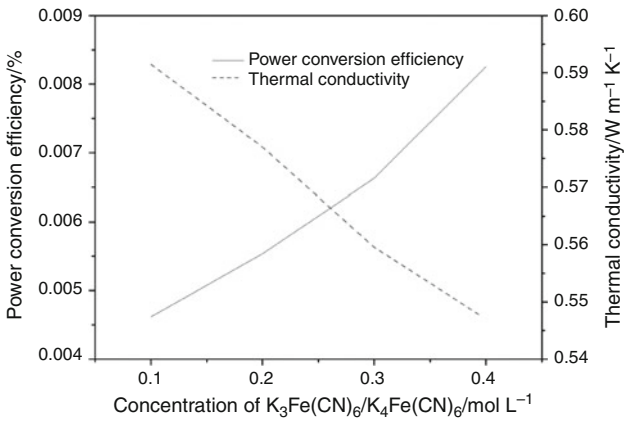

Fig. 5 Power conversion efficiency and thermal conductivity at increasing concentrations of $K_3Fe(CN)_6/K_4Fe(CN)_6$

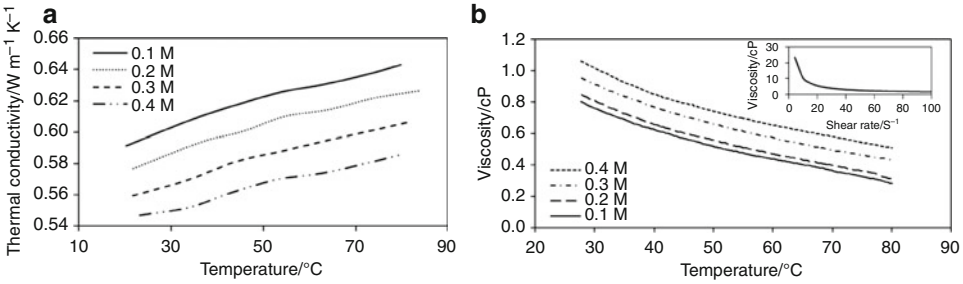

Fig. 6 **a** Thermal conductivity. **b** Viscosity vs. temperature of various concentrations of $K_3Fe(CN)_6/K_4Fe(CN)_6$ inset: viscosity at various shear rates for 0.4 M $K_3Fe(CN)_6/K_4Fe(CN)_6$

cells. The thermal conductivity for the 0.4 M solution ranges from 0.547 W/m K (at room temperature) up to 0.586 W/m K (at 80 °C), values that are lower than the minimum thermal conductivity of the 0.1 M solution which ranges from 0.591 W/m K (at room temperature) to 0.643 W/m K (at 80 °C). The lower thermal conductivity in the 0.4 M $K_3Fe(CN)_6/K_4Fe(CN)_6$ solution inhibits the thermal flux from the hot to the cold electrode and maximizes the power conversion efficiency by allowing a larger thermal gradient to be maintained between the two electrodes.

Viscosity measurements of the various concentrations of $K_3Fe(CN)_6/K_4Fe(CN)_6$ were performed to understand the trend of thermal conductivity obtained; i.e. thermal conductivity is inversely proportional to concentration but directly proportional to temperature. To establish the shear rate, an initial experiment was done using a concentration of 0.4 M, wherein the shear rate was varied from 1 to 100 s^{-1} while measuring the viscosity. The results shown in the inset of Fig. 6b indicate that after a shear rate of 70 s^{-1} the changes in viscosity are negligible. The viscosity of various concentrations of $K_3Fe(CN)_6/K_4Fe(CN)_6$ solutions was measured between temperatures of 25–80 °C using the established shear rate of 100 s^{-1} and are shown in Fig. 6b. It can be seen that an increase in concentration of the redox mediator causes a rise in viscosity of the solutions. Since heat transfer in liquids is dominated by convection, increased viscosity would impede the flow of the convective currents resulting in lower thermal conductivity for greater concentrations of the redox mediator. Furthermore, an increase in temperature results in a drop in the viscosity for all concentrations of $K_3Fe(CN)_6/K_4Fe(CN)_6$ solutions. In order for a molecule to escape from its neighbours and move in a liquid, it must possess a minimum amount of energy. Raising the temperature decreases the time molecules spend in contact with their nearest neighbours which is caused by the increased speed of molecules in the liquid. In short, intermolecular forces of attraction are offset by higher molecular kinetic energy at higher temperatures and this allows the liquid to flow more freely. This is consistent with Eq. 4, which depicts the temperature dependence of the coefficient of viscosity (which is inversely proportional to the mobility of molecules in a liquid) [28].

$$\eta \propto e^{\frac{Ea}{RT}} \tag{4}$$

where η is the coefficient of viscosity, Ea is the activation energy, R is the universal gas constant and T is the temperature.

For a thermogalvanic cell to produce a high mass power density and operate at high efficiency, the reaction products formed at the hot side must travel (via diffusion and convection) to the cold side and vice versa. The unavailability of ferrocyanide at the hot anode and ferricyanide at the cold cathode will result in lower values of I_d; i.e. mass transfer across the electrolyte will not occur fast enough to sustain the redox reactions in the cell. Despite the fact that an increase in concentration of the redox mediator in the electrolyte increases the viscosity, which hinders mass transport via convection, the mass power density of the thermogalvanic cell increases. The increased electrical conductivity of the electrolyte (292 ms at 0.4 M as compared to 63.4 ms at 0.1 M), shown in Fig. 7 reduces the ohmic overpotential in the cell and has a greater effect on the overall cell performance than mass transfer. This is evidenced by the scaling of mass power density with the redox mediator concentration.

The maximum mass power density obtained using R-GO electrodes was 25.51 W/kg at a temperature difference of 60 °C and a concentration of 0.4 M $K_3Fe(CN)_6/K_4Fe(CN)_6$. For platinum electrodes the maximum power

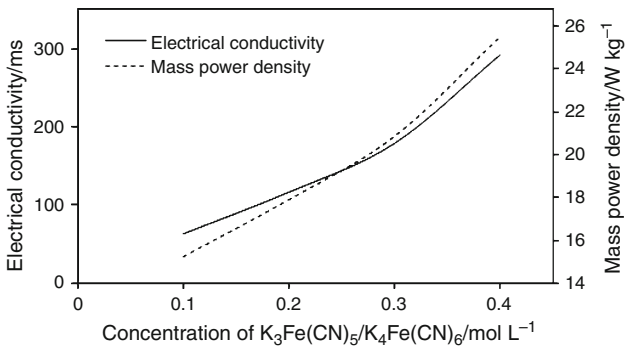

Fig. 7 Electrical conductivity and mass power density at increasing concentrations of $K_3Fe(CN)_6/K_4Fe(CN)_6$

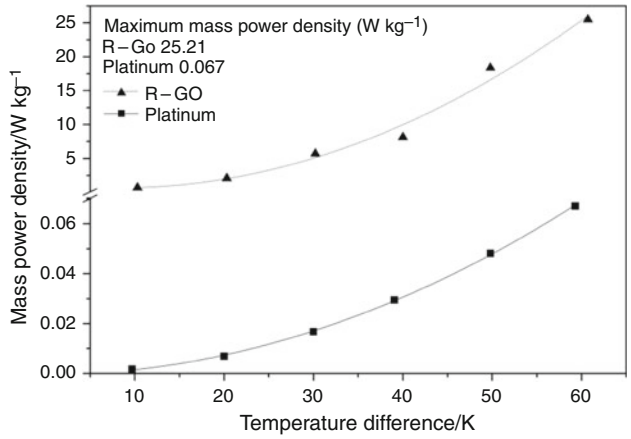

Fig. 8 Mass power density obtained using platinum and R-GO

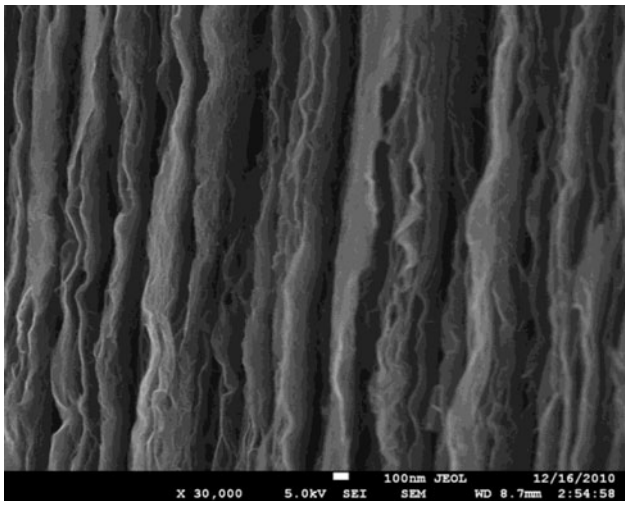

Fig. 9 Cross section of the R-GO film

density obtained was only 0.067 W/kg, a value lower by three orders of magnitude (shown in Fig. 8).

The higher mass power density obtained when using the R-GO electrode can be attributed to its porous structure. This can be seen in Fig. 9, which shows the cross section of the R-GO film.

Further evidence of the porous nature of the R-GO electrode is shown in Fig. 10a which depicts the higher I_d generated when the R-GO electrode was used (1207.37 A/kg) as compared to the platinum electrode (3.12 A/kg) at a temperature difference of 60 °C. The higher I_d is attributed to the larger electroactive surface area of R-GO. The V_{oc} for both materials (Fig. 10b) follows the same profile, wherein the Seebeck coefficients obtained are 1.47 mV/°C and 1.41 mV/°C for platinum and R-GO, respectively. This is expected since V_{oc} is not dependent on the electrode material but rather on the thermodynamics of the redox couple [3]. The fact that V_{oc} is the same for both materials indicates that the increase in power density is induced by the increased I_d obtained when R-GO electrodes are used.

A convenient method of standardizing power conversion measurements is to compare values obtained to that of a Carnot engine operating between the same temperatures and is given as:

$$\Phi_r = \frac{\Phi_{\text{thermogalvanic cell operating at } \Delta T}}{\Phi_{\text{Carnot engine operating at } \Delta T}} \quad (5)$$

This makes possible accurate comparison of different thermoelectric converters having different operating conditions, i.e. temperature difference, electrolyte used, etc. [3]. Using R-GO electrodes and an electrolyte concentration of 0.4 M the efficiency relative to a Carnot engine is 0.012%. This value is too low to be commercially viable however the thickness of the film (1.8 μm) must be taken into account. Thermal cell efficiency calculations are based on the geometric area and not the mass of the electrode (Eq. 3). Increasing the R-GO film thickness will result in a larger electroactive surface area (due to its porous nature), while maintaining the geometric area. It is surmised that this will result in larger values of I_d, power density and power conversion efficiency. Studies are currently being undertaken to confirm this.

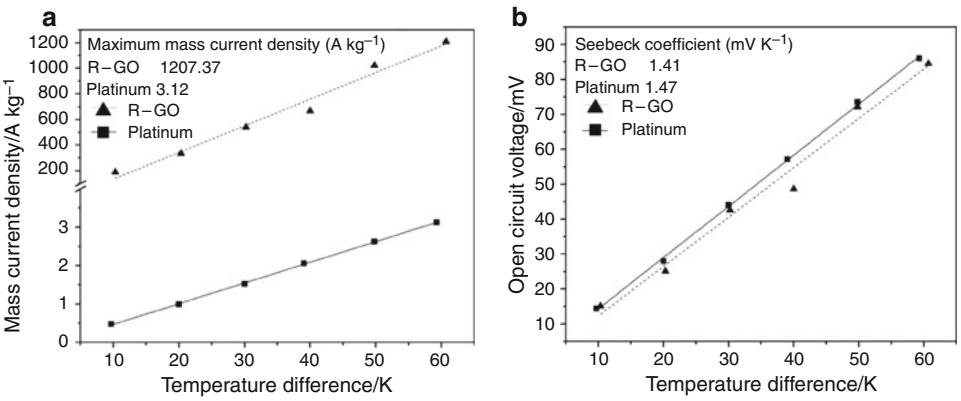

Fig. 10 **a** Mass current density. **b** Open circuit voltage generated using platinum and R-GO electrodes

Conclusions

Increasing the concentration of the $K_3Fe(CN)_6/K_4Fe(CN)_6$ redox mediator results in a decrease of the thermal conductivity of the electrolyte which maximizes the temperature gradient between the two electrodes. Despite the fact that viscosity scales with concentration which hinders mass transport between the two electrodes, the decrease in the ohmic overpotential (as electrolyte concentration is increased) has a greater effect on the thermal cell performance which results in higher short circuit currents produced, which leads to better mass power density. The synergistic effect of these factors results in improved power conversion efficiency of the thermal cell. R-GO is a feasible electrode material for thermogalvanic cells as it produces high mass power density due to its large electroactive surface area.

Acknowledgements The authors gratefully acknowledge funding from C-THERM TECHNOLOGIES for presentation of this work, the Department of Science and Technology, Philippines, and the ARC Centre of Excellence for Electromaterials Science.

References

1. Quickenden TI, Mua Y. The power conversion efficiencies of a thermogalvanic cell operated in three different orientations. J Electrochem Soc. 1995;142(11):3652–9.
2. Ratkje SK, Ikeshoji T, Syverud K. Heat and internal energy changes at electrodes and junctions in thermocells. J Electrochem Soc. 1990;137(7):2088–95.
3. Quickenden TI, Mua Y. A review of power generation in aqueous thermogalvanic cells. J Electrochem Soc. 1995;142(11):3985–94.
4. Goncalves R, Ikeshoji T. Comparative studies of a thermoelectric converter by a thermogalvanic cell with a mixture of concentrated potassium ferrocyanide and potassium ferricyanide aqueous solutions at great temperature differences. J Braz Chem Soc. 1992;3(3):4.
5. Noam L. Energy resources and use: the present (2008) situation and possible sustainable paths to the future. Energy. 2010;35(6):2631–8.
6. Fronk BM, Neal R, Garimella S. Evolution of the transition to a world driven by renewable energy. J Energy Res Technol. 2010;132(2):21009–15.
7. Vining CB. An inconvenient truth about thermoelectrics. Nat Mater. 2009;8(2):83–5.
8. Hertz HG, Ratkje SK. Theory of thermocells. J Electrochem Soc. 1989;136(6):1698–704.
9. Hornut JM, Storck A. Experimental and theoretical analysis of a thermogalvanic undivided flow cell with two aqueous electrolytes at different temperatures. J Appl Electrochem. 1991;21(12):1103–13.
10. Mua Y, Quickenden TI. Power conversion efficiency, electrode separation, and overpotential in the ferricyanide/ferrocyanide thermogalvanic cell. J Electrochem Soc. 1996;143(8):2558–64.
11. Li D, et al. Processable aqueous dispersions of graphene nanosheets. Nat Nano. 2008;3(2):101–5.
12. Khan U, et al. High-concentration solvent exfoliation of graphene. Small. 2010;6(7):864–71.
13. Lee C, et al. Measurement of the elastic properties and intrinsic strength of monolayer graphene. Science. 2008;321(5887):385–8.
14. Wang N, et al. The investigation of thermal conductivity and energy storage properties of graphite/paraffin composites. J Therm. Anal. Calorim. 2012;107:949–54.
15. Bolotin KI, et al. Ultrahigh electron mobility in suspended graphene. Solid State Commun. 2008;146(9–10):351–5.
16. Stoller MD, et al. Graphene-based ultracapacitors. Nano Lett. 2008;8(10):3498–502.
17. Eizenberg M, Blakely JM. Carbon monolayer phase condensation on Ni(111). Surf Sci. 1979;82(1):228–36.
18. Novoselov KS, et al. Electric field effect in atomically thin carbon films. Science. 2004;306(5696):666–9.
19. Coleman JN. Liquid-phase exfoliation of nanotubes and graphene. Adv Funct Mater. 2009;19(23):3680–95.
20. Park S, et al. Colloidal suspensions of highly reduced graphene oxide in a wide variety of organic solvents. Nano Lett. 2009;9(4):1593–7.
21. C-Therm Technologies Ltd.C-Therm Technologies-Products. http://www.ctherm.com/products/tci_thermal_conductivity.
22. Lerf A, et al. Structure of graphite oxide revisited. J Phys Chem B. 1998;102(23):4477–82.
23. Stankovich S, et al. Synthesis of graphene-based nanosheets via chemical reduction of exfoliated graphite oxide. Carbon. 2007;45(7):1558–65.
24. da Silva M, et al. Synthesis and characterization of CeO_2–graphene composite. J Therm Anal Calorim. 2012;107(1):257–63.
25. Hu R, et al. Harvesting waste thermal energy using a carbon-nanotube-based thermo-electrochemical cell. Nano Lett. 2010;10(3):838–46.
26. Artjom VS. Theoretical study of thermogalvanic cells in steady state. Electrochim Acta. 1994;39(4):597–609.
27. Quickenden TI, Vernon CF. Thermogalvanic conversion of heat to electricity. Sol Energy. 1986;36(1):63–72.
28. Atkins P, Paula Jd. Physical chemistry. New York: Oxford University Press; 2002.